Lifetime Determinations for Nuclei $A=10$, 11, and 12 from Gamma-Ray Doppler Shifts*

E. K. WARBURTON, J. W. OLNESS, K. W. JONES, C. CHASMAN, AND R. A. RISTINEN
Brookhaven National Laboratory, Upton, New York

AND

D. H. WILKINSON
Brookhaven National Laboratory, Upton, New York
and
Nuclear Physics Laboratory, Oxford, England

(Received 11 April 1966)

The Doppler-shift-attenuation technique was used to investigate the lifetimes of excited states of Be^{10}, B^{10}, B^{11}, C^{11}, and C^{12}. Gamma rays from nuclear levels populated by d, He^3, and α bombardment of thick Be and Cu-Be targets were detected with a lithium-drifted germanium detector at both forward and backward directions relative to the incident beam direction. Lifetimes were then extracted by comparing the differences in the Doppler shift as measured with the two targets. Gamma-ray peaks from Be^9+d were observed for the Be^{10} 5.96 $\rightarrow$ 3.37, Be^{10} 3.37 $\rightarrow$ 0, B^{10} 3.59 $\rightarrow$ 0.72, and B^{10} 5.16 $\rightarrow$ 2.15 transitions and mean lifetimes of $<0.8\times10^{-13}$ sec, $(1.6\pm0.3)\times10^{-13}$ sec, $(1.20\pm0.43)\times10^{-13}$ sec, and $<0.8\times10^{-13}$ sec were obtained for the initial states of these transitions. The Doppler shift of the C^{12} 4.43 $\rightarrow$ 0 transition was investigated using the $Be^9(\alpha,n)C^{12}$ reaction. A mean lifetime of $(5.7_{-1.7}^{+2.3})\times10^{-14}$ sec was obtained for the C^{12} 4.43-MeV level. Levels in B^{11} and C^{11} were formed by the $Be^9(He^3,p)B^{11}$ and $Be^9(He^3,n)C^{11}$ reactions, and upper limits were set for the mean life-times of five levels in these nuclei. The strengths of known transitions from the B^{10} 2.15- and 3.59-MeV levels are discussed in terms of the independent-particle model. The agreement is found to be generally good for the 3.59-MeV level and poor for the 2.15-MeV level. Several experimental and theoretical points remain to be clarified.

I. INTRODUCTION

WE have investigated the Doppler shifts of gamma-ray transitions in Be^{10}, B^{10}, B^{11}, C^{11}, and C^{12}. These transitions were induced by bombardment of Be^9 targets with d, α, and He^3 beams. The motive for undertaking this work was to obtain further knowledge of electromagnetic transition rates in the $A=10$ nuclei, and the emphasis of this paper is therefore placed on the investigation of transition rates in Be^{10} and B^{10}. As part of this work we have re-examined a previous determination[1] of the lifetime of the Be^{10} 3.37-MeV level using an improved analysis procedure and also taking account of the recently discovered[2,3] fact that the Be^{10} 5.96-MeV "level" is in fact a doublet. We also report on a lifetime measurement for the first-excited state of C^{12} which was performed, primarily, to test our procedure. Some Doppler shift measurements leading to lifetime limits for some states in B^{11} and C^{11} are also presented.

The nuclei $A=10$, lying midway along the $1p$ shell, are interesting and "complicated." From the early days of independent-particle-model (IPM) calculations[4,5] it has been clear that a rather surprisingly good account can be afforded of these nuclei by the IPM from the point of view of the level schemes. It has, however, more recently become apparent[6] that the radiative transitions can not be accounted for by the IPM[7] for the same values of the intermediate coupling parameter a/K that give the satisfactory account of the level schemes and that the only approach towards agreement between the experimental and theoretical versions of the gamma-ray branching ratios is at values of a/K so low as to be completely unacceptable. This disagreement inspired a recent detailed examination[8] of the radiative properties of the 5.16- and 4.77-MeV $J^\pi=2^+$ $T=1$ and $J^\pi=3^+$ $T=0$ states of B^{10} with the object of determining absolute radiative widths to make the disagreement with the IPM quantitative. In the present paper then we continue this program with measurements on the 3.59-MeV $J^\pi=2^+$ $T=0$ state of B^{10}. We had also hoped to measure the lifetime of the 2.15-MeV $J^\pi=1^+$, $T=0$ state of B^{10}. In this we were unsuccessful. However, the lifetime of this state has recently been determined elsewhere,[9] and we shall discuss the radiative properties of both the 2.15- and 3.59-MeV levels of B^{10}. Figure 1 shows the states of B^{10} and the transitions of chief interest in this work.

Since this program of experimental classification was begun progress has also been made with the IPM. The IPM to which we have referred so far takes the traditional approach in which the intermediate coupling parameter a/K and the exchange integral K of the

* Work performed under the auspices of the U. S. Atomic Energy Commission.

[1] E. K. Warburton, D. E. Alburger, and D. H. Wilkinson, Phys. Rev. **129**, 2180 (1963).

[2] F. C. Young, P. D. Forsyth, M. L. Roush, and W. F. Hornyak, in *Nuclear Spin-Parity Assignments*, edited by N. B. Gove and R. L. Robinson (Academic Press Inc., New York, 1966), pp. 179–182.

[3] E. K. Warburton and D. E. Alburger, in Ref. 2, pp. 114–145.

[4] D. R. Inglis, Rev. Mod. Phys. **25**, 390 (1953).

[5] D. Kurath, Phys. Rev. **101**, 216 (1956).

[6] E. K. Warburton, D. E. Alburger, and D. H. Wilkinson, Phys. Rev. **132**, 776 (1963).

[7] D. Kurath, Phys. Rev. **106**, 975 (1957).

[8] D. E. Alburger, D. J. Bredin, P. D. Parker, D. H. Wilkinson, P. F. Donovan, A. Gallmann, R. E. Pixley, L. F. Chase, Jr., and R. E. McDonald, Phys. Rev. **143**, 692 (1966).

[9] J. A. Lonergan and D. J. Donahue, Phys. Rev. **139**, B1149 (1965); **145**, 998(E) (1966).

effective residual nucleon-nucleon interaction are the only operative variables, all other relevant parameters being guessed and frozen at the beginning of the calculation. This we call IPM_{old}. The new approach, IPM_{new}, takes all matrix elements of the effective residual nucleon-nucleon interaction, 15 in the $1p$-shell, as its parameters and determines them and also two necessary single-particle energies by the simultaneous fitting of the entire body of "certain" data on the level schemes. In the more recent[10] of the two versions of IPM_{new},[10,11] separate fittings were made using $A=6$ through 16, $IPM_{new(6)}$, and using $A=8$ through 16, $IPM_{new(8)}$. It appears[8] that IPM_{new} may give a distinctly superior account of the $M1$ transitions than IPM_{old}, and this comparison and also the discussion of $E2$ widths are continued in this paper.

We here deal chiefly with transitions, for B^{10}, between states of $T=0$ so the $M1$ transitions are expected to be weak, while the $E2$ transitions that commonly mix with them may enjoy the usual collective enhancement. The experimental situation is therefore often a complicated one, requiring determinations of the $E2/M1$ mixing ratio before comparison with the theoretical values for either $M1$ or $E2$ transition strengths may be made. The well-known failure of the IPM to predict sufficiently strong $E2$ rates still persists in IPM_{new} and so its absolute predictions are not to be taken seriously in themselves. However, it is commonly found experimentally that the collective effects operate in the sense that they amplify the $E2$ strength already provided by the IPM, as of course is automatically assured by the weak-surface-coupling or effective-charge formalism for parametrizing the collective effects. Although the effective charge formalism cannot be literally interpreted deep into the $1p$ shell, it seems that it usually remains an empirically valid way of describing the transitions.[12] It is therefore interesting to continue to ask whether strong experimental $E2$ transitions are associated with strong $E2$ transitions of the model and the predictions of IPM_{new} on this point are therefore compared with experiment.

II. EXPERIMENTAL PROCEDURE

Levels of B^{10} and Be^{10} were populated through the reactions $Be^9(d,n)B^{10}$ ($Q=4.362$ MeV) and $Be^9(d,p)Be^{10}$ ($Q=4.590$ MeV). Gamma rays were detected with a lithium-drifted germanium gamma-ray spectrometer with a sensitive volume of 3 cm^3. Two target positions were provided 84 cm apart with the Ge(Li) detector midway between them, so that gamma rays emerging at forward and backward angles to the beam could be detected without moving the detector. Two types of targets were used, beryllium metal and copper-beryllium alloy (Cu-Be) containing 15 at.% of Be. Both targets were thick enough to stop the 2.8-MeV deuteron beam. Except that the Ge(Li) detector replaces a NaI(Tl) crystal, this experimental arrangement is identical to that used in a previous measurement,[1] performed at this laboratory, on the lifetime of the 3.37-MeV level of Be^{10}.

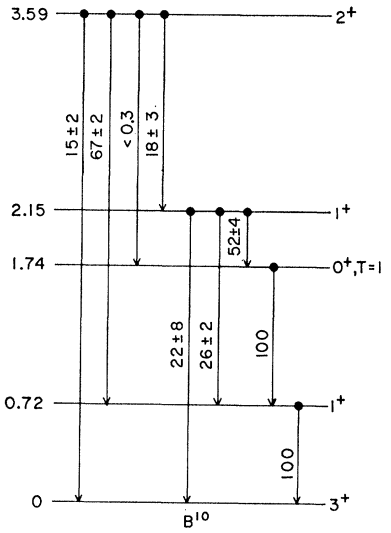

FIG. 1. Level scheme of B^{10} and transitions of chief interest in this work, from information collected in Ref. 14.

The gamma-ray spectra were recorded with a 1024-channel pulse-height analyzer. A pulse-height dispersion of 1.36 keV per channel was achieved by the use of a post-bias amplifier in conjunction with this analyzer. The pulse-height spectra covered the energy range between about 1.2 and 2.5 MeV.

Two sets of data were taken, the first with a ThC″ source (2.614-MeV gamma ray) for calibration and the second with a Co^{60} source (1.332-MeV gamma ray) for calibration. A data set consisted of the spectra from Be and Cu-Be targets for gamma rays emitted in both the forward and backward directions. For detection of these gamma rays the average angles (θ) to the beam direction were such that $\cos\theta=0.991$ in the first case and -0.987 in the second (i.e., $\cos\theta_1-\cos\theta_2=1.978$).

The two spectra recorded using the Be target and the Co^{60} source are shown in Fig. 2, while similar spectra from the Cu-Be target are shown in Fig. 3. In both cases the lower and upper curves show the spectra of gamma rays emitted in the forward and backward directions, respectively. The Be spectra were recorded with a beam intensity of 0.15 μA. The beam current for the Cu-Be spectra was 1 μA. With these beam currents the analyzer dead-time for the two targets was identical.

The identification of the gamma-ray lines in Figs. 2 and 3 is based on previous studies of the gamma rays from Be^9+d at this laboratory.[1,6,13] In analyzing the results due cognizance was taken of the suspected or

[10] S. Cohen and D. Kurath, Nucl. Phys. **73**, 1 (1965); and private communication from D. Kurath.
[11] D. Amit and A. Katz, Nucl. Phys. **58**, 338 (1964).
[12] E. K. Warburton, D. E. Alburger, D. H. Wilkinson, and J. M. Soper, Phys. Rev. **129**, 2191 (1963).
[13] D. J. Bredin, J. W. Olness, and E. K. Warburton, Bull. Am. Phys. Soc. **9**, 407 (1964).

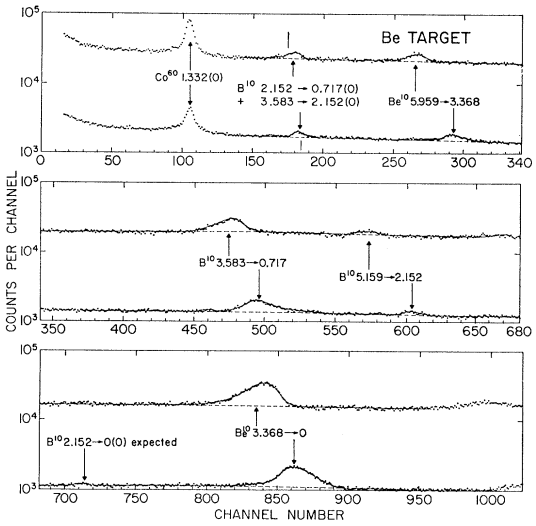

FIG. 2. Ge(Li) spectra of gamma-ray lines from 2.8-MeV deuteron bombardment of a thick Be target. The data were obtained with a dispersion of 1.36 keV per channel and include the energy region from 1.2 to 2.5 MeV. The lower and upper curves are for detection of gamma rays in the forward and backward directions, respectively. The gamma-ray peaks are identified by the nucleus and the initial and final states to which they are assigned. Two escape peaks are unmarked while full-energy loss peaks are designated by (0). The vertical lines in the top part of the figure show the expected centroids of the 3.583 → 2.152(0) peaks, while the arrows give the calculated centroids of the composite 2.152 → 0.717(0)+3.583 → 2.152(0) peaks.

known presence of other possible transitions.[14] The gamma-ray lines of Figs. 2 and 3, with the exception of the Co^{60} calibration line and perhaps those originating from the B^{10} 2.15-MeV level, all show the expected Doppler broadening. We find that two transitions in Be^{10} and two in B^{10} give peaks which are isolated and intense enough so that their Doppler shifts can be calculated. These data provide little useful information on the B^{10} 2.15-MeV level. The expected position of the B^{10} 2.15 → 0 full-energy-loss peak is indicated in Figs. 2 and 3. This peak is probably present but is too weak to give any reliable information. The full-energy-loss peaks of the B^{10} 2.15 → 0.72 and B^{10} 3.59 → 2.15 transitions (see Fig. 1) are unresolved and are calculated to be of roughly comparable intensity. Thus we can only say that the percentage Doppler shift of the 2.15 → 0.72 transition is considerably less than that of the four prominent transitions shown in Figs. 2 and 3 which indicates that the lifetime of the B^{10} 2.15-MeV level is considerably longer than that of, say, the B^{10} 3.59-MeV level. This conclusion is consistent with the lifetime measurement of Lonergan and Donahue.[9] The C^{13} 3.085 → 0 transition apparent in Fig. 3 shows no detectable Doppler shift but appreciable Doppler broadening, which indicates that this line originates primarily from a C^{12} contamination of the slit system and not from the target.

The detector resolution in the present experiment was about 10 keV full-width at half-maximum (FWHM) for the Th*C*″ 2.614-MeV two-escape peak, while the FWHM for the Be^{10} 3.37 → 0 two-escape peak in Figs. 2 and 3 is about 35 keV. Thus the detector resolution is small compared to the width of the Doppler-broadened peaks for all the observed Be^{10} and B^{10} lines except those originating from the B^{10} 2.15-MeV level. The line shapes evident in Figs. 2 and 3 are due to several effects all of which are folded together. The most important are the kinematic effects due to (1) the angular distribution of the (d,n) or (d,p) reaction products and (2) the variation in deuteron energy which ranges from 2.8 MeV to the threshold for production of a given gamma-ray line. For the four prominent B^{10} and Be^{10} lines there is very little (if any) difference between the widths measured with the two targets, which indicates that the structure of these lines is dominated by the kinematic effects. Another source of line structure is that associated with the effect we are utilizing—namely, the slowing down of the recoiling Be^{10} or B^{10} nuclei in the stopping material. If the emission velocity is defined as the recoil ion velocity at the moment of gamma-ray emission, it is clear that the slowing down process gives rise to a distribution of emission velocities lying between the extrema of zero and the maximum recoil velocity allowed by the reaction kinematics. The shape of this distribution, and thus the resultant energy distribution of the gamma rays emitted, is determined by the rela-

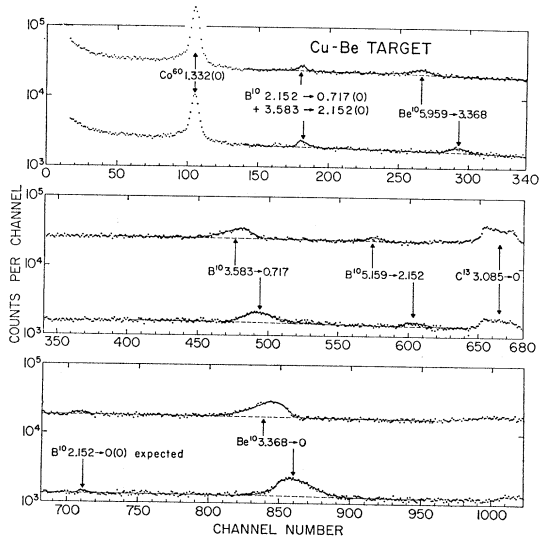

FIG. 3. Ge(Li) spectra of gamma-ray lines from 2.8-MeV deuteron bombardment of a thick Cu-Be target. The data were obtained with a dispersion of 1.36 keV per channel and include the energy region from 1.2 to 2.5 MeV. The lower and upper curves are for detection of gamma rays in the forward and backward directions, respectively. The gamma-ray peaks are identified by the nucleus and the initial and final states to which they are assigned. Two escape peaks are unmarked while full-energy loss peaks are designated by (0).

[14] T. Lauritsen and F. Ajzenberg-Selove, Nucl. Phys. **78**, 1 (1966); F. Ajzenberg-Selove and T. Lauritsen, Nucl. Phys. **11**, 1 (1959).

tionship between the nuclear lifetime and the rate with which the recoiling nuclei lose energy in the stopping material.

It is thus clear that the significant quantity to be extracted from a given spectrum is the *average* energy of a given line rather than the energy associated with the peak yield. For a detector resolution broad compared to the natural line structure the distinction between the average energy and the energy associated with the peak yield is small and often negligible as long as the detector response is symmetric about the peak.[15] (This was true for the previous[1] study of the Be^{10} 3.37 → 0 transition, for which case the detector [NaI(Tl)] resolution of ~200 keV was much greater than the line widths evident in Figs. 2 and 3.) For the highly asymmetric line shapes of Figs. 2 and 3, however, the average energy is quite different from the peak energy. By definition, the average energy is obtained by finding the centroid of the peak, and this is the method we have used. The centroids were obtained with a computer program which fitted an exponential to a given pulse-height region on each side of a line (the straight lines of Figs. 2 and 3), interpolated this background under the gamma-ray lines (the dashed straight lines of Figs. 2 and 3), subtracted this background from the original data, and found the centroid of a given pulse height region of the remainder.

We note further that the structure associated with a given gamma-ray line is expected to be symmetric with respect to a plane at right angles to the beam direction. That is, for detection at 90° to the beam the natural line shape is symmetric with respect to the average energy and for equal angles on each side of 90° the line shapes must also be identical if one of them is inverted about its average energy. This symmetry was found to be quite accurately obeyed by the spectra taken at forward and backward angles in the present work. There were, however, some slight deviations from this symmetry which could be explained by the detector response which is known to give rise to a small low-energy tail. This asymmetry in the detector response was taken into account with negligible error in the analysis of the data.

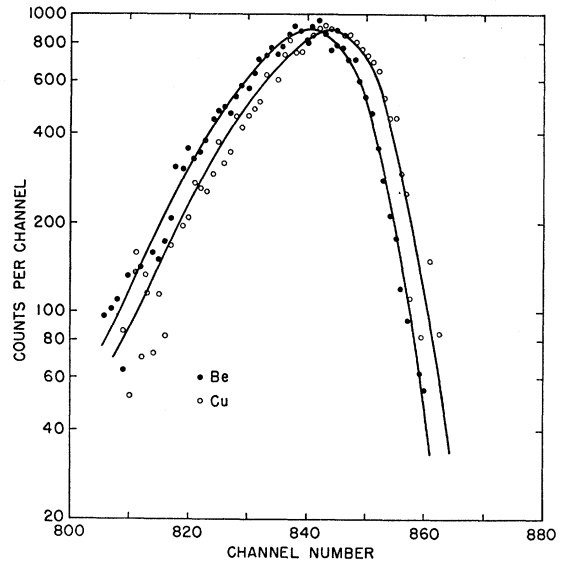

FIG. 4. The two-escape peak of the Be^{10} 3.37 → 0 transition observed in the backward direction following bombardment of a Be target (closed circles) and Cu-Be target (open circles) with 2.8-MeV deuterons. The data are those of Figs. 2 and 3 with background subtracted. The curves drawn through the points have nearly identical shapes but are shifted by 3 channels relative to each other. It appears that the peak for the Cu-Be target is slightly narrower than that for the Be target.

[15] A. E. Litherland, M. J. L. Yates, B. M. Hinds, and D. Eccleshall, Nucl. Phys. 44, 220 (1963).

TABLE I. Resume of B^{10} and Be^{10} Doppler shifts from Be^9+d for the Be target (ΔE_{Be}) and the Cu-Be target (ΔE_{Cu}).

Transition (MeV)	ΔE_{Cu} (keV)	ΔE_{Be} (keV)	$R_F'(=\Delta E_{Cu}/\Delta E_{Be})$
Be^{10} 5.959 → 3.368	36.3±1.0	36.3±1.0	1.00±0.035
B^{10} 3.583 → 0.717	26.5±0.7	32.5±0.7	0.82±0.025
B^{10} 5.159 → 2.152	39.0±1.0	39.8±1.0	0.98±0.035
Be^{10} 3.368 → 0	28.1±0.7	36.1±0.7	0.78±0.025

The shapes of the four prominent lines measured with the Be and Cu-Be targets were practically indistinguishable. A typical example illustrating this is shown in Fig. 4, which shows the two-escape peak of the Be^{10} 3.37 → 0 transition (with background subtracted) obtained in the backward direction from both the Be and Cu-Be targets. The similarity of the line shapes and the difference in centroids (~3 channels) due to the different stopping materials is apparent from this figure.

The information of interest obtained from analysis of the various spectra is collected in Table I. The second and third columns of this table give the differences in the average energies (ΔE) of the four gamma-ray transitions considered for detection in the forward and backward directions. The second column gives the results for the Cu-Be target, the third column gives the shifts for the Be target, and the fourth column gives the ratio of the two, i.e., $R_F'(=\Delta E_{Cu}/\Delta E_{Be})$. The uncertainties assigned to the results of Table I include the statistical uncertainties, but arise primarily from systematic errors such as that associated with the background subtraction and long-term gain stabilities. (The latter was monitored by the Co^{60} or ThC″ peak.) The systematic errors were estimated from the reproducibility of the results, from possible errors involved in the procedure for finding the centroids, and from the uncertainties due to the presence of known or possible gamma rays other than those identified in Figs. 2 and 3. The relative insensitivity of the centroid determination to the limits defined in the computations was tested by deliberately varying these limits and observing the change in the computed centroid values. We note here that the B^{10} 3.59 → 2.15 peak intensity (see Fig. 2) has a 2.8%

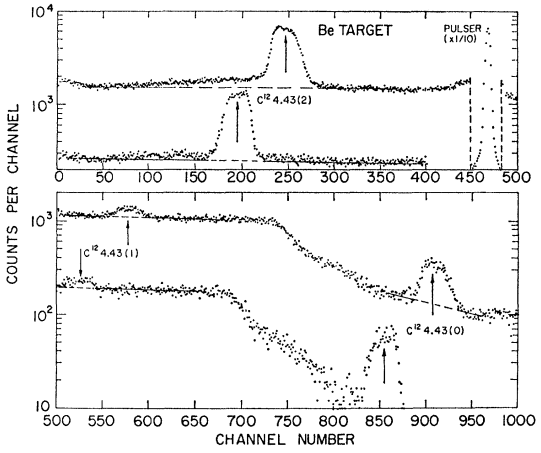

FIG. 5. Ge(Li) spectra showing the C^{12} 4.43-MeV gamma ray from 3.2-MeV α-particle bombardment of a thick Be target. The data were obtained with a dispersion of 1.55 keV per channel. The upper and lower curves are for detection of gamma rays in the forward and backward directions, respectively. The full-energy-loss, one-escape and two-escape peaks of the C^{12} 4.43-MeV gamma ray are identified, as is the pulser peak in one of the two spectra. The spectrum for the forward direction is displaced upwards by a factor of 2.

component due to feeding from the 5.16 → 3.59 cascade transition. This value was determined from the intensity of the 5.16 → 2.15 peak (Fig. 2) where the relative intensities of the two branches from the 5.16-MeV level were taken as (5.16 → 3.59)/(5.16 → 2.15) = 7/44. Since the lifetime of the B^{10} 5.16-MeV level is much less than that of the B^{10} 3.59-MeV level, the presence of this component has a negligible influence on the quoted value of R_F' for the 3.59 → 2.15 transition.

The data listed in Table I will be analyzed in the next section to obtain limits or estimates for the lifetimes of the four initial states involved.

The Doppler shift of the C^{12} 4.43 → 0 transition was investigated using an experimental arrangement identical to that described above. The $Be^9(\alpha,n)C^{12}$ ($Q=5.704$ MeV) reaction was used to populate the first-excited state of C^{12} at a bombarding energy of 3.2 MeV. The data were accumulated as described above except that an electronic pulser provided the reference line. Three sets of four spectra each were accumulated. Two of these spectra are shown in Fig. 5. Doppler shifts were determined for the full-energy-loss, one-escape, and two-escape peaks apparent in this figure. Thus, in all, nine determinations of the ratio R_F' were obtained for the 4.43 → 0 transition. These were in excellent agreement and gave an average value of 0.920±0.008 based on a difference in the shift between the Be and Cu-Be targets of 4.0±0.4 channels. This result is more accurate than that obtained for the B^{10} and Be^{10} gamma rays because of the improved statistics, i.e., 12 spectra rather than four, and because the ratio of Doppler shift to line width is considerably larger for the C^{12} results (compare Figs. 2 and 5).

The method used for the measurements of the B^{10}, Be^{10}, and C^{12} Doppler shifts was also applied to the study of some ground-state transitions in B^{11} and C^{11} using the $Be^9(He^3,p)B^{11}$ ($Q=10.325$ MeV) and $Be^9(He^3,n)C^{11}$ ($Q=7.560$ MeV) reactions with a bombarding energy of 3.2 MeV. One set of four spectra was recorded. The two spectra obtained using the Be target are illustrated in Fig. 6. The relative intensities of the various lines and the energies of the transitions were found to be consistent with previous work.[14,16] The results of the analysis of these spectra are listed in Table II. In the fourth column of Table II are listed the Doppler shifts predicted for very short lifetimes assuming an average He^3 beam energy of 2.8 MeV and an isotropic distribution of the outgoing protons or neutrons in the (He^3,p) or (He^3,n) reaction. The uncertainties attached to these calculated Doppler shifts correspond to ±0.2 MeV in the average beam energy and ±0.33 in $\langle\cos\theta_{c.m.}\rangle$, where $\theta_{c.m.}$ is the angle of the proton or neutron to the beam axis in the center-of-mass system and $\langle\cos\theta_{c.m.}\rangle$ is the average value of $\cos\theta_{c.m.}$.

TABLE II. Resumé of B^{11} and C^{11} Doppler shifts from Be^9+He^3 for the Be target (ΔE_{Be}) and the Cu-Be target (ΔE_{Cu}).

Transition (MeV)	ΔE_{Cu} (keV)	ΔE_{Be} (keV)	ΔE_{max} (keV)	$R_F'(=\Delta E_{Cu}/\Delta E_{Be})$
C^{11} 6.35 → 0	115.4±5	112.3±3.3	140±31	1.03±0.05
C^{11} 6.49 → 0	126.4±10	135.0±6.6	143±31	0.94±0.08
B^{11} 6.76 → 0	152.0±10	152.1±6.6	149±43	1.00±0.08
C^{11} 6.90 → 0	147.2±5	151.8±3.3	152±31	0.97±0.04
B^{11} 7.30 → 0	149.6±5	146.5±3.3	161±47	1.02±0.04

The results given in Table II will be analyzed in the next section to obtain upper limits on the mean lifetimes of the B^{11} and C^{11} levels involved.

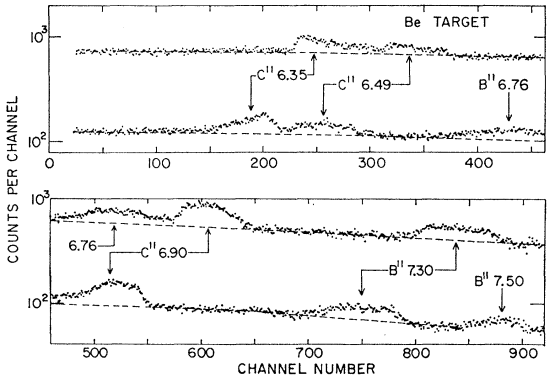

FIG. 6. Ge(Li) spectra of two-escape peaks from 3.2-MeV He^3 bombardment of a thick Be target. The data were obtained with a dispersion of 1.66 keV per channel and include the energy region from 5.0 to 6.6 MeV. The upper and lower curves are for detection of gamma rays in the forward and backward directions, respectively. The gamma rays, all of which correspond to ground-state transitions, are identified by the nucleus and the initial state to which they are assigned. The lower curves are displaced downwards by a factor of 5.

[16] J. W. Olness, E. K. Warburton, D. E. Alburger, and J. A. Becker, Phys. Rev. **139**, B512 (1965).

III. ANALYSIS

A. Stopping-Power Data

The first step in the analysis of the experimental results (Table I) was to construct stopping-power curves for the stopping of Be and B nuclei in Ni and Be. Since very little experimental data is available for the stopping of Be and B ions, the stopping-power curves were obtained by interpolation of existing stopping-power and charge-state data for other ions. Nickel was chosen for the calculations since the stopping power of nickel for various ions has been extensively measured and its stopping power is quite close to that of the Cu-Be alloy. The stopping-power and charge-state data cited in the recent review article of Northcliffe[17] as well as that cited by Warburton *et al.*[1] were used in these interpolation procedures.

Figures 7 and 8 illustrate the results obtained for Be and B ions stopping in Ni and Be. The stopping power is plotted versus ion velocity in units of $c/137$ (i.e., $v_0=c/137$) so that the curves are valid for all isotopes of Be and B. The interpolation was performed for discrete values of v/v_0 as shown by the data points in Figs. 7 and 8. The error bars attached to these points show our estimates of the combined uncertainties of the experimental data and the interpolation procedure. The dashed curves in Figs. 7 and 8 are fits to the functional form, $dE/dx=K_e(v/v_0)$, while the solid curves are fitted to the expression

$$\frac{dE}{dx}=K_n/(v/v_0)+K_e(v/v_0)-K_3(v/v_0)^3 \qquad (1)$$

by adjusting the constants K_n, K_e, and K_3. This latter expression fits the dE/dx data for Ni quite well for $v/v_0\leq 6$ but fails to fit the dE/dx data for stopping in Be for $v/v_0\gtrsim 2.5$. The leading term in Eq. (1) gives rise to the upturn of dE/dx at low decreasing values of v/v_0 in Fig. 7. There is scanty experimental evidence for this term from measurements of dE/dx. However, there is theoretical evidence for a term giving a similar effect and also experimental evidence for such a term from measurements of ion ranges.[1,17]

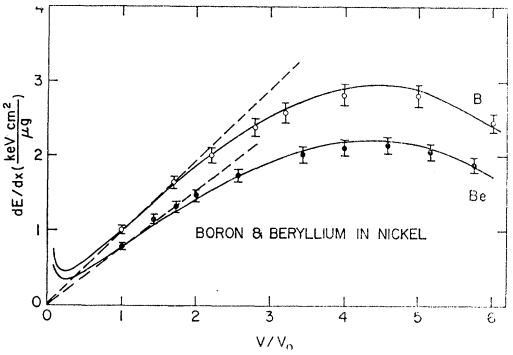

FIG. 7. Stopping power curves for B and Be ions in Ni showing differential energy loss as a function of ion velocity (in units of $v_0=c/137$). The data points were obtained by interpolation as explained in the text. The dashed curves are a fit of $dE/dx=K_e(v/v_0)$ to the region $1.0\leq v/v_0\leq 1.8$ while the full curves are a fit of $dE/dx=K_n/(v/v_0)+K_e(v/v_0)-K_3(v/v_0)^3$ to the region $1.0\leq v/v_0\leq 6$. For B ions the dashed curve corresponds to $K_e=0.96\pm 0.05$ while the full curve corresponds to $K_n=0.05$, $K_e=0.96$, and $K_3=0.016$. For Be ions the dashed curve corresponds to $K_e=0.78\pm 0.04$ while the full curve corresponds to $K_n=0.04$, $K_e=0.75$, and $K_3=0.013$. All constants are in units of (keV cm²)/μg.

[17] L. C. Northcliffe, Ann. Rev. Nuc. Sci. 13, 67 (1963).

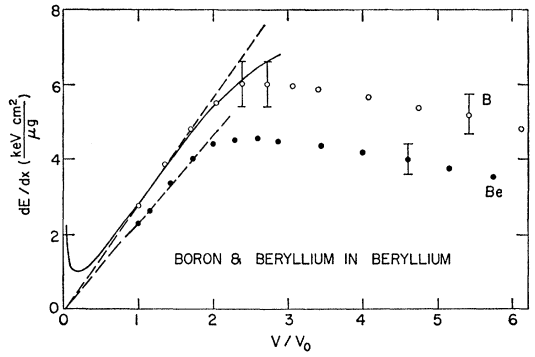

FIG. 8. Stopping power curves for B and Be ions in Be showing differential energy loss as a function of ion velocity (in units of $v_0=c/137$). The data points were obtained by interpolation as explained in the text. The dashed curves are a fit of $dE/dx=K_e(v/v_0)$ to the region $1.0\leq v/v_0\leq 1.8$ while the full curve for B ions is a fit of $dE/dx=K_n/(v/v_0)+K_e(v/v_0)-K_3(v/v_0)^3$ to the region $1.0\leq v/v_0\leq 2.7$. The dashed curves for B and Be correspond to $K_e=2.84\pm 0.15$ and 2.3 ± 0.15, respectively; while the full curve for B ions corresponds to $K_n=0.08$, $K_e=2.84$, and $K_3=0.053$. All constants are in units of (keV cm²)/μg.

The dE/dx curves of Figs. 7 and 8 were used to obtain a relationship between the nuclear lifetimes and the Doppler-shift-attenuation factor F'. For $dE/dx=K_e(v/v_0)$ this is a simple procedure which gives $F'=\lambda\alpha/(1+\lambda\alpha)$ where α is the characteristic slowing-down time of the ion in the stopping material and $\lambda=\tau^{-1}$, where τ is the mean lifetime of the nuclear state emitting the gamma radiation. If dE/dx is not proportional to (v/v_0), then F' will be a function of the initial velocity v_i of the moving ion. In this case a curve of τ versus F' can be constructed from a dE/dx curve by numerical integration, if v_i is well defined.[15] This method is not very well-suited to the present experiment since we are dealing with a continuous range of initial ion velocities. For this reason we have chosen to fit the dE/dx curves with Eq. (1) and to solve for F' analytically.

The expression for dE/dx given in Eq. (1) results in the following expressions for the ion range R (in cm):

$$R=\alpha\left[\left(\frac{2}{\pi}\right)v_m\tanh^{-1}\left(\frac{\pi}{2}\frac{v}{v_m}\right)-\left(\frac{2}{\pi}\right)v_n\tan^{-1}\left(\frac{\pi}{2}\frac{v}{v_n}\right)\right], \qquad (2)$$

where $v_m=(\pi/2)(K_e/K_3)^{1/2}v_0$, $v_n=(\pi/2)(K_n/K_e)^{1/2}v_0$, and the characteristic slowing-down time α is given (in sec) by

$$\alpha=mv_0/K, \qquad (3)$$

with $K=(K_e^2+4K_nK_3)^{1/2}$, and m the mass of the moving ion. The Doppler-shift-attenuation factor F' corresponding to Eq. (1) can be expressed in the form

$$F'=\frac{\lambda\alpha}{2}\frac{(1+C_i)^{1/2}}{C_i^{(\lambda\alpha+1)/2}}\int_0^{C_i}\frac{x^{(\lambda\alpha-1)/2}dx}{(1+x)^{1/2}}, \tag{4}$$

where

$$C_i=\frac{K-K_e+2K_3(v_i/v_0)^2}{K+K_e-2K_3(v_i/v_0)^2}. \tag{5}$$

The integral in Eq. (4) can be solved numerically, expressed as a rapidly-converging power series in C_i, or solved exactly for integral values of $\lambda\alpha$. For $K_3=0$ or both K_3 and $K_n=0$, Eqs. (2) and (4) reduce to expressions given previously for R and F'.[1]

B. The Be^{10} 3.37-MeV Level

We now consider the information which can be obtained from the Doppler shifts given in Table I. We consider first the Be^{10} 3.37 → 0 transition. The earlier Doppler shift measurements[1] performed at this laboratory gave results which, transformed to the geometry and convention appropriate to Table I, are $\Delta E_{Cu}=27.9\pm0.8$ keV, $\Delta E_{Be}=(34.5\pm0.7)$ keV, and $R_F'=0.81\pm0.028$, in satisfactory agreement with the present results. We adopt an average of the two determinations of R_F', 0.795 ± 0.025. In the previous analysis the functional form for dE/dx of Eq. (1) was assumed with $K_3=0$. This introduced very little error since the recoiling B and Be ions have $v/v_0\leq2.5$ in the present experiment, as in the previous one, and with this condition the effect of a nonzero K_3 is quite small.

Our present analysis is, therefore, identical to that described previously, except that we no longer set $K_3=0$ and we take $R_F'=0.795\pm0.025$ rather than $R_F'=0.81\pm0.028$. These two changes practically cancel each other so that the lifetime quoted previously[1] for the Be^{10} 3.37-MeV level as obtained by the Be, Cu-Be comparison method is practically unchanged.

In the previous study[1] the lifetime of the Be^{10} 3.37-MeV level was also obtained by a second method which was dependent upon a knowledge of the Doppler shift of the Be^{10} 5.96 → 3.37 cascade. This shift had been inferred previously from measurements on the Doppler shift of the Be^{10} 5.96 → 0 transition with a result which would be (42 ± 1.7) keV for the present geometrical arrangement. This is to be compared to the direct observations listed in Table I of $\Delta E_{Cu}=36.3\pm1.0$ keV. The discovery[2,3] that the Be^{10} 5.96-MeV "level" is a $J^\pi=2^+$, 1^- doublet separated by 1.1 ± 0.4 keV invalidates the previous analysis, since the two states are formed approximately equally by the $Be^9(d,p)Be^{10}$ reaction and the 1^- state decays mainly by a ground-state decay while the 2^+ state decays mainly by cascade via the 3.37-MeV level. In fact, the difference between the percentage Doppler shift presently determined for the 5.96 → 3.37 transition and that reported previously for the 5.96 → 0 transition can be taken as supporting evidence for the presence of a doublet level at 5.96 MeV in B^{10}. We can now use the present determination for the Doppler shift of the 5.96 → 3.37 transition to properly analyze the previous[1] results. We note that the value of R_F' obtained for this transition is consistent with unity so that we need not consider the lifetime of the $J^\pi=2^+$, 5.96-MeV level in this analysis. Furthermore, although small admixtures of the $J^\pi=1^-$ 5.96 → 3.37 transition in the $J^\pi=2^+$ 5.96 → 3.37 transition are allowed,[2,3] the possibility of such an admixture introduces negligible uncertainty in the analysis because the percentage Doppler shifts of the 5.96 → 0 and 5.96 → 3.37 transitions are not too different. Accordingly, we have re-analyzed the results of the second method of the previous[1] work, using for this purpose the results listed in Table I for the Be^{10} 5.96 → 3.37 transition.

The value given previously for the mean lifetime of the Be^{10} 3.37-MeV level was $(1.4\pm0.3)\times10^{-13}$ sec. Our re-analysis changes this value slightly, yielding a final revised value for the mean lifetime of

$$\tau(Be^{10}\ 3.37\text{-MeV level})=(1.6\pm0.3)\times10^{-13}\ \text{sec}.$$

An independent determination of the lifetime of the Be^{10} 3.37-MeV level has recently been reported from Doppler-shift measurements using the $Li^7(Li^7,\alpha)Be^{10}$ reaction.[18] This result gives $\tau=(2.2\pm0.4)\times10^{-13}$ sec, which is somewhat higher than our present value but is nevertheless in fair agreement with it. We adopt

$$\tau(Be^{10}\ 3.37\text{-MeV level})=(1.9\pm0.3)\times10^{-13}\ \text{sec},$$
$$\Gamma_\gamma(Be^{10}\ 3.37\text{-MeV level})=(3.5\pm0.6)\times10^{-3}\ \text{eV}$$

for the average values of the mean lifetime and radiative width based on all Doppler-shift measurements performed on the Be^{10} 3.37 → 0 transition.

C. The B^{10} 3.59-MeV Level

We now consider the B^{10} 3.59 → 0.72 transition. The fact that R_F' for this transition is practically identical to that for the Be^{10} 3.37 → 0 transition means that the two transitions have nearly equal values of $\lambda\alpha$. This is so because to an accuracy well within that of the stopping-power data of Figs. 7 and 8 the dE/dx curves for B and Be ions are proportional to each other for $v/v_0\leq2.5$ and the proportionality constant is the same for stopping in Be and Ni.

The lifetime estimate obtained from the measurement of R_F' will be an insensitive function of the distribution of initial ion velocities assumed. Very little information is available on either the excitation function for formation of the 3.59-MeV level or on the (d,n) angular distributions for various deuteron energies between 0 and 2.8 MeV—these being the measurements needed to arrive at a knowledge of the distribution of initial ion

[18] G. C. Morrison, J. E. Evans, N. H. Gale, R. W. Ollerhead, and E. K. Warburton (unpublished).

velocities. Thus we have assumed that the distribution of initial ion velocities is the same for the reactions $Be^9(d,n)B^{10*}$ (3.59-MeV level) and $Be^9(d,p)Be^{10*}$ (3.37-MeV level) and have included in the lifetime calculation our estimate of the uncertainty introduced by this assumption. With this assumption we find that the relationship between the R_F' values obtained for the Be^{10} $3.37 \rightarrow 0$ and B^{10} $3.59 \rightarrow 0.72$ transitions leads to

$$\tau(B^{10}\ 3.59\text{-MeV level}) = (0.64 \pm 0.22) \times \tau(Be^{10}\ 3.37\text{-MeV level}).$$

Using our adopted value for the lifetime of the Be^{10} 3.37-MeV level, we obtain

$$\tau(B^{10}\ 3.59\text{-MeV level}) = (1.20 \pm 0.43) \times 10^{-13}\ \text{sec},$$
$$\Gamma_\gamma(B^{10}\ 3.59\text{-MeV level}) = (5.5 \pm 2.2) \times 10^{-3}\ \text{eV}.$$

The mean lifetime of the B^{10} 3.59-MeV level has been measured recently by Lonergan and Donahue[19] who obtained $(1.75 \pm 0.7) \times 10^{-13}$ sec, in fair agreement with the present result. The average of our measurement and this previous one[19] gives,

$$\tau(B^{10}\ 3.59\text{-MeV level}) = (1.45 \pm 0.4) \times 10^{-13}\ \text{sec},$$
$$\Gamma_\gamma(B^{10}\ 3.59\text{-MeV level}) = (4.5 \pm 1.3) \times 10^{-3}\ \text{eV}.$$

D. The B^{10} 5.16- and Be^{10} 5.96-MeV Levels

The measurements of R_F' for the B^{10} $5.16 \rightarrow 2.15$ and Be^{10} $5.96 \rightarrow 3.37$ transitions are both consistent with unity. This means that the lifetimes of the two initial states involved are quite short compared to the slowing down time in Cu-Be and Be and only upper limits can be given for these two levels. For both transitions we find that $\tau < 0.8 \times 10^{-13}$ sec corresponds to two standard deviations from the measured values of R_F'. The limit for the B^{10} 5.16-MeV level is consistent with its known properties.[14] The lifetime limit for the $5.96 \rightarrow 3.37$ transition applies to the $J=2$ member[2] of the 5.96-MeV doublet. This lifetime limit can be used to set upper limits on the possible admixtures of quadrupole radiation in the predominantly dipole $5.96 \rightarrow 3.37$ transition. We take the conservative limit $Z^2\Gamma_{\gamma W}$ for the largest possible strength of both $M2$ and $E2$ transitions, where $\Gamma_{\gamma W}$ is the Weisskopf estimate of the transition strength.[20] Combining this limit with the lower limit[3] of 90% on the branching ratio of the $J=2$, $5.96 \rightarrow 3.37$ transition and the present limit on the mean lifetime of this transition gives an upper limit of 0.48 for the intensity ratio $E2/M1$ for an even-parity assignment to the $J=2$, 5.96-MeV level. The corresponding limit for an odd-parity assignment to the $J=2$, 5.96-MeV level is 0.02 for the intensity ratio $M2/E1$. The limit on the possible amount of $M2$ radiation has been used[3] to fix the $J=2$, 5.96-MeV level as $J^\pi = 2^+$.

[19] J. A. Lonergan and D. J. Donahue, Bull. Am. Phys. Soc. **11**, 27 (1966); and private communication from D. J. Donahue.

[20] D. H. Wilkinson, in *Nuclear Spectroscopy*, edited by F. Ajzenberg-Selove (Academic Press Inc., New York, 1960), Part B, pp. 852–889.

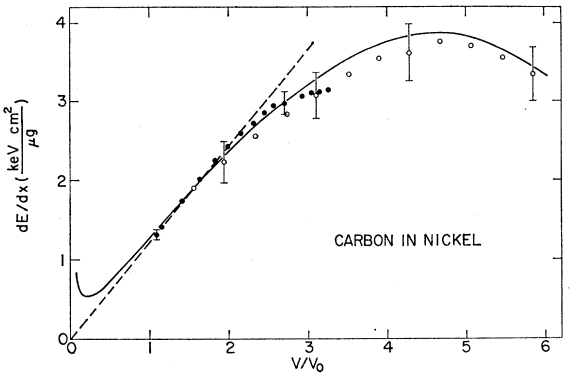

FIG. 9. Stopping power curve for C ions in Ni showing differential energy loss as a function of ion velocity (in units of $v_0 = c/137$). The solid points are data of D. I. Porat and K. Ramavataram [Proc. Phys. Soc. (London) **77**, 97 (1961)], while the open circles were obtained by interpolation as explained in the text. Representative uncertainties are indicated for the two sets of data points. The dashed curve is a fit of $dE/dx = K_e(v/v_0)$ to the region $1 \leq v/v_0 \leq 2$ while the full curve is a fit of $dE/dx = K_n/(v/v_0) + K_e(v/v_0) - K_3(v/v_0)^3$ to the region $1 \leq v/v_0 \leq 6$. The dashed curve corresponds to $K_3 = 1.23 \pm 0.06$ while the full curve corresponds to $K_n = 0.06$, $K_e = 1.24$, and $K_3 = 0.019$. All constants are in units of (keV cm²/μg).

E. The C^{12} 4.43-MeV Level

The analysis of the Doppler shift measurements for the C^{12} 4.43-MeV level followed the same procedure as was used for the Be^{10} 3.37-MeV level. The energy-loss curve for C^{12} ions stopping in Ni is shown in Fig. 9; a similar curve (not shown) was obtained for stopping in Be. The analysis in this case was relatively uncomplicated by effects due to deviation from the linear relationship $dE/dx = K_e(v/v_0)$. This was so because the lifetime is quite short, i.e., R_F' is large, and the maximum initial velocity of the recoiling ions which is allowed by the kinematics is $v/v_0 = 2.7$. Actually, the spread of initial velocities can be inferred from the line shape of the C^{12} 4.43-MeV two-escape peak (Fig. 5) and can be used to estimate the average correction for deviations from a linear dE/dx-versus-v/v_0 relationship. Other information used to estimate this effect are the excitation curve for production of the C^{12} 4.43-MeV gamma ray in the $Be^9(\alpha,n)C^{12}$ reaction[21,22] and angular distributions for the reaction.[22] The estimated deviation of R_F' from the value it would have for a linear dE/dx-versus-v/v_0 relationship is $(1 \pm 1)\%$. Note that the effect of the deviation in the two targets is largely cancelled when the ratio of the Doppler shifts in the two targets is taken. Our value of the mean lifetime and radiative width of the C^{12} 4.43-MeV level based on the present determination $R_F' = 0.920 \pm 0.008$ are

$$\tau(C^{12}\ 4.43\text{-MeV level}) = (5.7_{-1.7}^{+2.3}) \times 10^{-14}\ \text{sec},$$
$$\Gamma_\gamma(C^{12}\ 4.43\text{-MeV level}) = (11.5_{-3.2}^{+5}) \times 10^{-3}\ \text{eV}.$$

[21] T. W. Bonner, A. A. Kraus, Jr., J. B. Marion, and J. P. Schiffer, Phys. Rev. **102**, 1348 (1956).

[22] J. B. Garg, J. M. Calvert, and N. H. Gale, Nucl. Phys. **19**, 264 (1960); T. Retz-Schmidt, T. W. Bonner, G. U. Din, and J. L. Weil, Bull. Am. Phys. Soc. **5**, 110 (1960), and private communication from J. L. Weil.

The latest and most accurate value for the radiative width of this level from inelastic electron scattering is[23]

$$\Gamma_\gamma(e,e')=(11.2\pm1.2)\times10^{-3}\text{ eV},$$

while resonance fluorescence has yielded[24]

$$\Gamma_\gamma(\gamma,\gamma')=(10.5\pm2)\times10^{-3}\text{ eV}.$$

Although it is clear that the accuracy of our method is not very competitive with that of the other two, the excellent agreement of the three results increases our confidence in our analysis procedure.

F. Levels in B^{11} and C^{11}

The results listed in Table II lead to upper limits on the mean lifetimes for the two B^{11} and three C^{11} levels involved as follows:

C^{11} 6.35-MeV level: 1.1×10^{-13} sec,
C^{11} 6.49-MeV level: 2.5×10^{-13} sec,
B^{11} 6.76-MeV level: 3.0×10^{-13} sec,
C^{11} 6.90-MeV level: 1.6×10^{-13} sec,
B^{11} 7.30-MeV level: 1.0×10^{-13} sec.

These limits were obtained using the dE/dx curves for boron and carbon ions which have already been discussed. For the first and last of these transitions the limits correspond to three standard deviations from the measured values of R_F'. For the remaining three transitions more stringent limits are obtained (also to three standard deviations) from values of F_{Cu}' derived from the data of Table II (for the C^{11} 6.90-MeV level the two limits coincide). Which method gives the more stringent limit depends on the accuracy of the measurement and how close the measured Doppler shift (in both targets) is to the maximum shift allowed by the kinematics.

These limits (which are 99.7% confidence limits) on the mean lifetimes of these five states in B^{11} and C^{11} are consistent with, but more restrictive than, previously quoted limits of $\tau<5\times10^{-13}$ sec[16] for all five levels. Although these limits add little to our understanding of the nuclear spectroscopy of mass 11, they may prove useful in interpreting future spectroscopy studies and also in planning measurements of the mean lifetimes of these states.

IV. THE B^{10} 2.15- AND 3.59-MeV LEVELS: COMPARISON WITH THEORY

A. General

In this discussion we are concerned chiefly with transitions between states of $T=0$. All our states have the same parity. The $M1$ transitions will therefore suffer the usual isotopic-spin inhibition (with the exception of that between the 2.15-MeV $J^\pi=1^+$ state and the $J^\pi=0^+$ $T=1$ state at 1.74 MeV). The $E2$ transitions, since $\Delta T=0$, may show the usual collective enhancement common in the $1p$ shell. We may therefore expect significant $E2/M1$ ratios if the gamma-ray energy is at all high. For comparison with our experimental data we show in Table III the single-particle $(1p_{3/2}\rightarrow1p_{3/2})$ $E2$ radiative widths for transitions between the states with which we are concerned in this paper. These widths have been evaluated using $\langle r^2\rangle_p=7.9\times10^{-26}$ cm^2, a figure derived and used in a recent analysis.[12]

TABLE III. Single-particle $(1p_{3/2}\rightarrow1p_{3/2})$ $E2$ radiative widths in B^{10}.

Initial state (MeV)	Final state (MeV)	$\Gamma_{sp}(E2)$ (10^{-4} eV)
3.59	2.15	0.25
	0.72	7.7
	0	24.0
2.15	0.72	0.24
	0	1.87

It does not seem likely that $\langle r^2\rangle_p$ can be greater than 10×10^{-26} cm^2 at the most so the $E2$ single-particle unit could possibly be as much as 60% larger than that derived from $\langle r^2\rangle_p=7.9\times10^{-26}$ cm^2 with corresponding adjustment in the comparison between the IPM and experiment.

We may note that $E2$ widths for $\Delta T=0$ transitions range up to as much as 7 of these single-particle units[8] (for the 4.05-MeV transition between the 4.77-MeV and the 0.72-MeV states of B^{10}) and are typically 1 or 2 units; they can also be quite small.

B. The 3.59-MeV State

We combine our present data on the absolute width of the state with recent branching-ratio data[6,13,25,26] to find the partial absolute widths shown in Table IV.

Transition to the 2.15-MeV State

Comparison with Table III shows that the 1.44-MeV transition to the 2.15-MeV state must be essentially

TABLE IV. Radiative widths for the decay of the B^{10} 3.59-MeV level.

Final state (MeV)	Branching ratio[a] (%)	Absolute width (10^{-4} eV)
2.15	18±3	8.1±2.6
0.72	67±2	30 ±9
0	15±2	6.7±2

[a] We exclude the transition to the 1.74-MeV state reported (Ref. 25) as of relative intensity (10±5)% on account of its clearly lower abundance (<0.3%) in a search made explicitly for it (Ref. 26).

[23] H. L. Crannell and T. A. Griffy, Phys. Rev. **136**, B1580 (1964).
[24] V. K. Rasmussen, F. R. Metzger, and C. P. Swann, Phys. Rev. **110**, 154 (1958).
[25] W. F. Hornyak, C. A. Ludemann, and M. L. Roush, Nucl. Phys. **50**, 424 (1964).
[26] R. E. Segel, P. P. Singh, S. S. Hanna, and M. A. Grace, Phys. Rev. **145**, 736 (1966).

pure $M1$. The predictions for the partial $M1$ radiative widths are

$$\mathrm{IPM_{new(8)}}: 6.6\times10^{-4}\ \mathrm{eV};\quad \mathrm{IPM_{new(6)}}: 6.6\times10^{-4}\ \mathrm{eV}.$$

These predictions are in excellent agreement with experiment. The prediction from $\mathrm{IPM_{old}}$ is 0.64×10^{-4} eV which is in much worse agreement with experiment.

Transition to the 0.72-MeV State

Table III shows that we may here expect a substantial $E2$ component. The predictions for the strengths of the $M1$ component are

$$\mathrm{IPM_{new(8)}}: 7.7\times10^{-4}\ \mathrm{eV};\quad \mathrm{IPM_{new(6)}}: 1.9\times10^{-4}\ \mathrm{eV}.$$

$\mathrm{IPM_{new}}$ can therefore only be reconciled with the experimental data if indeed the $E2/M1$ ratio is high. It seems possible that this may be the case. The "multipole meter" results[3,27] require $|x|>0.7$ where x is the $E2/M1$ amplitude ratio. Angular-correlation studies of the $3.59\rightarrow0.72\rightarrow0$ cascade[28] give a slight preference for the regions $0.12<|x|<0.45$ or $|x|>6$. These data together then favor $|x|>6$, which is just about acceptable with an $M1$ component on the low side of the predictions of $\mathrm{IPM_{new}}$. However, as may be seen from Table III, this would then imply a strong $E2$ component for this transition, about 4 single-particle units. This $E2$ transition would then be about as strong as the remarkable one of strength 7 single-particle units between the 4.77- and 0.72-MeV states.[8] Further work on the correlation measurements or other methods of fixing the $E2/M1$ ratio would evidently be well worthwhile.

If all present data are correct, we have in this transition a rather weak $M1$ and a strong $E2$. We should therefore inquire of $\mathrm{IPM_{new}}$ whether it predicts a strong $E2$ component in this case since; as noted in Sec. I, the collective $E2$ enhancements usually seem to operate in the sense of speeding up transitions that are already strong in the IPM. In the effective-charge formalism the effects of collective motion are caricatured by ascribing to the neutrons a charge of x electronic units and to the protons a charge $1+x$. For $E2$ transitions of the type $T=0\rightarrow T=0$ such as concern us in this discussion this has the effect of multiplying the straight IPM prediction for the $E2$ radiative width by the factor $(1+2x)^2$. The value $x=0.5$ was used in a parallel study[8] of the 4.77-MeV and 5.16-MeV states of B^{10} and we shall adopt this value. Thus for purposes of presentation we will quote the straight IPM prediction $\Gamma_\gamma(E2)$ and also the enhanced prediction $\Gamma_\gamma'(E2)=4\Gamma_\gamma(E2)$. However, we note that the value $x=0.5$ was arrived at from a comparison[12] between the IPM and the experimental value of $(1.4\pm0.3)\times10^{-13}$ sec for the Be^{10} 3.37-MeV level which gave $x=0.5\pm0.2$. This analysis, when combined with our presently adopted value of $(1.9\pm0.3)\times10^{-13}$ sec for the mean lifetime of the Be^{10} 3.37-MeV level, gives $x=0.4\pm0.2$. Thus, it should be kept in mind that the values quoted for $\Gamma_\gamma'(E2)$ may over-estimate the collective enhancement. For the transition now under discussion we have the prediction

$$\mathrm{IPM_{new(8)}}:\ \Gamma_\gamma(E2)=8.7\times10^{-4}\ \mathrm{eV};\quad \Gamma_\gamma'(E2)=35\times10^{-4}\ \mathrm{eV}.$$

The prediction of $\mathrm{IPM_{new(6)}}$ is about 4% lower.

We see that $\mathrm{IPM_{new}}$ indeed predicts this to be a very strong $E2$ transition, 1.1 single-particle units unenhanced, and that the enhanced prediction is in good accord with experiment if, as experiment suggests, the $E2/M1$ ratio is high.

We may note that this strong $E2$ and the very strong $E2$ between the 4.77- and 0.72-MeV states[8] make the $J^\pi=1^+$, 2^+, 3^+ states at 0.72, 3.59, and 4.77 MeV reminiscent of a $K=1$ rotational band. Similarly the very strong $E2$ between the $J^\pi=4^+$ state at 6.02 MeV and the ground state[8] may suggest the beginning of a $K=3$ band. However these bands, if they are to be so identified, are evidently rather impure.

The prediction of $\mathrm{IPM_{old}}$ as to the $M1$ width is 39×10^{-4} eV which would strongly disagree with experiment if indeed the $E2/M1$ ratio is high, but is in good agreement with a low value of $E2/M1$.

Transition to the Ground State

Table III shows that this transition may well be predominantly $E2$. The results of the "multipole meter" measurements[27] are consistent with pure $E2$ radiation and require $|x|>0.45$. The prediction as to the $M1$ radiative widths are

$$\mathrm{IPM_{new(8)}}: 10\times10^{-4}\ \mathrm{eV};\quad \mathrm{IPM_{new(6)}}: <0.3\times10^{-4}\ \mathrm{eV}.$$

The IPM predictions as to the $E2$ width are

$$\mathrm{IPM_{new(8)}}:\ \Gamma_\gamma(E2)=5.5\times10^{-4}\ \mathrm{eV};\quad \Gamma_\gamma'(E2)=22\times10^{-4}\ \mathrm{eV}.$$

The prediction of $\mathrm{IPM_{new(6)}}$ is about 7% higher. These predictions are in good accord with experiment, particularly if the $E2/M1$ ratio is high.

Our data are inconsistent with $\mathrm{IPM_{old}}$ which predicts an $M1$ width of 78×10^{-4} eV for this transition.

TABLE V. Radiative widths for the decay of the B^{10} 2.15-MeV level.

Final state (MeV)	Branching ratio (%)	Absolute width (10^{-4} eV)
1.74	52±4	$0.69_{-0.21}^{+0.47}$
0.72	26±2	$0.34_{-0.11}^{+0.24}$
0	22±8	$0.29_{-0.1}^{+0.2}$

[27] E. K. Warburton, D. E. Alburger, A. Gallmann, P. Wagner, and L. F. Chase, Jr., Phys. Rev. **133**, B42 (1964).
[28] S. M. Shafroth and S. S. Hanna, Phys. Rev. **104**, 399 (1956).

C. The 2.15-MeV State

We combine the radiative width of $(1.3_{-0.4}{}^{+0.9})\times10^{-4}$ eV measured for this state by Lonergan and Donahue[9] with the branching ratios taken from the literature[25,26,29] to find the partial absolute widths shown in Table V.

Transition to the 1.74-MeV State

This transition is a pure $M1$ uninhibited by isotopic spin. This may be compared directly with the IPM prediction for the $M1$ transition width:

$$\mathrm{IPM_{new(8)}}: 9.2\times10^{-4}\ \mathrm{eV};\quad \mathrm{IPM_{new(6)}}: 5.6\times10^{-4}\ \mathrm{eV}.$$

Agreement is quite poor. It would be interesting to know whether $\mathrm{IPM_{new}}$ can accommodate a slower transition.

$\mathrm{IPM_{old}}$ predicts a radiative width of 25×10^{-4} eV which disagrees more strongly with experiment.

Transition to the 0.72-MeV State

Table III shows that there may be a sizeable $E2$ component in this transition. Preliminary results of Lonergan and Donahue[19] indicate the intensity ratio of $E2$ to $M1$ radiation is either less than 0.016 or greater than 64.

The predictions as to the $M1$ rates are

$$\mathrm{IPM_{new(8)}}: 10\times10^{-4}\ \mathrm{eV};\quad \mathrm{IPM_{new(6)}}: 3.4\times10^{-4}\ \mathrm{eV}.$$

These figures are considerably higher than experiment and so would favor the lower $E2/M1$ ratio. $\mathrm{IPM_{old}}$ is equally unsuccessful: It predicts a radiative width of 7.8×10^{-4} eV. The IPM predictions as to the $E2$ component are

$$\mathrm{IPM_{new(8)}}: \Gamma_\gamma(E2)=2.4\times10^{-6}\ \mathrm{eV};\quad \Gamma_\gamma'(E2)=0.1\times10^{-4}\ \mathrm{eV}$$

$$\mathrm{IPM_{new(6)}}: \Gamma_\gamma(E2)=6.2\times10^{-6}\ \mathrm{eV};\quad \Gamma_\gamma'(E2)=0.25\times10^{-4}\ \mathrm{eV}.$$

The $\Gamma_\gamma'(E2)$ are in good agreement with experiment and thus favor a high $E2/M1$ ratio. Thus, the $M1$ prediction is in poor agreement with experiment for either $E2/M1$ ratio (<0.016 or >64) but favors the lower value, while the $E2$ rate is in satisfactory agreement for $E2/M1>64$ but in poor agreement for $E2/M1<0.016$. We note that the ambiguity in the $E2/M1$ ratio cannot be removed by any presently feasible experimental techniques so that it would appear that this discrepancy must be investigated from the theoretical side.

Transition to the Ground State

This transition is $E2$ and so may be compared directly with $\mathrm{IPM_{new}}$. Table III shows that its strength is quite small, about 0.14 single particle units. The IPM predictions are

$$\mathrm{IPM_{new(8)}}: \Gamma_\gamma(E2)=0.13\times10^{-4}\ \mathrm{eV};\quad \Gamma_\gamma'(E2)=0.5\times10^{-4}\ \mathrm{eV}$$

$$\mathrm{IPM_{new(6)}}: \Gamma_\gamma(E2)=0.17\times10^{-4}\ \mathrm{eV};\quad \Gamma_\gamma'(E2)=0.66\times10^{-4}\ \mathrm{eV}.$$

These predictions are in good agreement with experiment.

D. Summary of Discussion

We have found that $\mathrm{IPM_{new}}$ is consistently more successful than $\mathrm{IPM_{old}}$. Some questions concerning the decay of the $J^\pi=1^+$ 2.15-MeV level have suggested themselves for $\mathrm{IPM_{new}}$:

(a) Can it accommodate a slower transition to the 1.74-MeV state?

(b) Can it accommodate a slower $M1$ transition to the 0.72-MeV state?

(c) How sensitive to the details of the calculation is the $E2$ transition rate to the 0.72-MeV state?

Some experimental questions concerning the decay of the $J^\pi=2^+$ 3.59-MeV state have emerged from our discussion:

(a) What is the $E2/M1$ mixing ratio in the transition to the 0.72-MeV state?

(b) What is the $E2/M1$ mixing ratio in the ground-state transition?

ACKNOWLEDGMENTS

We are grateful to D. Kurath for making available to us unpublished results on the $E2$ strengths in the IPM, to J. L. Weil for sending us unpublished results for the $Be^9(\alpha,n)C^{12}$ reaction, to P. Paul and S. S. Hanna for calling our attention to an initially erroneous analysis of the Doppler shift of the B^{10} $2.15\rightarrow0.72$ transition, and to D. J. Donahue for communication of unpublished results.

[29] E. L. Sprenkel and J. W. Daughtry, Phys. Rev. **124**, 854 (1961).